Research Article

Toru Akasofu*, Masanobu Kusakabe, Shin'ichi Takeda, and Shigeru Tamaki

Structural evidence of complex formation in liquid Pb–Te alloys

https://doi.org/10.1515/htmp-2020-0064
received April 6, 2020; accepted June 2, 2020

Abstract: The former analysis of the structural data in liquid Pb–Te alloys, based on the neutron diffraction measurements for this system, was insufficient to obtain the microscopic and spatial configurations in this system. In order to obtain these configurations, we have newly analyzed by using the Reverse Monte Carlo simulations and the method of Voronoi polyhedron. The partial structure factors $S_{ij}(Q)$ and thereby $g_{ij}(r)$ are newly estimated by using the former data of neutron diffraction measurements, which are now exactly reproduced by the obtained total structure factors $S(Q)$. From these results, it is concluded that the liquid $Pb_{0.5}Te_{0.5}$ is spatially configured by the mixture of some sorts of covalent-type formation of PbTe molecules and dissociated Pb and/or Te ions with conduction electrons, which result is completely consistent with results of electrical resistivity measurements and also with the thermodynamic analysis.

Keywords: liquid Pb–Te, complex formation, structure, neutron diffraction, Reverse Monte Carlo

1 Introduction

Nowadays, the solid compound lead telluride PbTe is an important material in view of industrial technology, and in due course, its atomic and electronic structures are fully investigated [1]. As a result, the solid lead telluride PbTe has a rock salt type structure with mainly a weak covalent bonding as one of the narrow gap semiconductors.

On melting of this solid lead telluride PbTe, there occurs a small volume expansion like a similar phenomenon in a usual solid–liquid transition, because of a decrease in density and the increase in concentration fluctuations. Naturally, this material in its liquid state, more or less, is thought to have remained in the same bonding character, that is, mainly remaining in the covalent-type bonding.

Earlier, on the other hand, we had serially investigated the electronic behaviors in liquid VIb-Te alloys [2–4]. The most interesting information obtained from various electronic properties of these liquid alloys was the existence of the complex- or compound-forming effect, which gave several anomalous tendencies in their concentration dependences on typical electronic properties such as electrical resistivity and the magnetic susceptibility. In order to certify this complex formation in liquid Pb–Te alloy, we are also studying the thermodynamic properties of this system, based on a model of the mixture of covalent molecules of PbTe and metallic part of Pb–Te binary alloys [5].

Since both the electronic behavior and the thermodynamic one in liquid Pb–Te binary alloys have therefore strongly indicated the covalent-type formation of PbTe molecule, we have to clarify the existing evidence of this formation from the structural information. Many years ago, this concept had prompted us to report the structure of liquid Pb–Te binary alloys. And such an investigation has been preliminarily reported in the form of a university bulletin [6]. However, our former analysis was insufficient to reveal what happened in the liquid Pb–Te alloys, and at that time we had no technique known nowadays, as the Reverse Monte Carlo simulation which is a powerful method to know the three dimensional and short-range configurations of the constituent atoms in liquids. Under these situations, we have newly analyzed the former experimental data on the structures of liquid Pb–Te binary alloys, in order to reveal the real microscopic feature of the covalent-type formation of PbTe molecule.

* **Corresponding author: Toru Akasofu,** Department of Engineering, Niigata Institute of Technology, Kashiwazaki 9451195, Japan, e-mail: mikikimi@shore.ocn.ne.jp
Masanobu Kusakabe: Department of Engineering, Niigata Institute of Technology, Kashiwazaki 9451195, Japan
Shin'ichi Takeda: Department of Physics, Kyushu University, Fukuoka 8190385, Japan
Shigeru Tamaki: Department of Physics, Niigata University, Niigata 9502181, Japan

2 A brief review on the experimental procedure and results

Although the experimental procedure and the obtained results on the neutron diffraction for liquid Pb–Te binary alloys have preliminarily been reported in a university bulletin [6], we will adopt them to discuss our present purpose. The alloy compositions investigated by neutron diffraction were $Pb_{1-c}Te_c$, with $c = 0$, 0.2, 0.4, 0.5, 0.6, 0.8 and 1.0, respectively. Each sample was sealed into a thin quartz tube under a vacuum of 1.3×10^{-4} Pa. The diffraction apparatus of the Institute for Solid State Physics, Tokyo University, at JRR-3 was used. Using the coherent neutron scattering intensity per atom, the total scattering intensity $I(Q)$ was obtained.

The observed structure factor, $S^{obs}(Q)$, of each binary alloy can be written as follows,

$$S^{obs}(Q) = \frac{I(Q) - \langle b^2\rangle - \langle b^2\rangle}{\langle b^2\rangle} = w_{Pb-Pb}S_{Pb-Pb}(Q) + w_{Pb-Te}S_{Pb-Te}(Q) + w_{Te-Te}S_{Te-Te}(Q)$$
$$\langle b^2\rangle = c_{Pb}b_{Pb}^2 + c_{Te}b_{Te}^2 \quad \langle b\rangle = c_{Pb}b_{Pb} + c_{Te}b_{Te}, \tag{1}$$

and

$$w_{Pb-Pb} = \frac{c_{Pb}^2 b_{Pb}^2}{\langle b^2\rangle}, \quad w_{Pb-Te} = \frac{2c_{Pb}c_{Te}b_{Pb}b_{Te}}{\langle b^2\rangle},$$
$$w_{Te-Te} = \frac{c_{Te}^2 b_{Te}^2}{\langle b^2\rangle},$$

and $Q = (4\pi/\lambda)\sin\theta$.

The notation b_i is the coherent scattering amplitude of the element i, which is obtainable from the list presented by Bacon [7]. Here, c_{Pb} and c_{Te} are the atomic fractions of the constituents, and b_{Pb} and b_{Te} are the atomic scattering amplitudes of Pb and Te nucleus, respectively. Along with the concentration method [8], we assume that the partial structure factor between atoms i and j, $S_{ij}(Q)$ is not changed with the concentration of $c_{Pb} = (1 - c_{Te})$.

The partial structure factor $S_{ij}(Q)$ is defined by the generalized equation as follows,

$$S_{ij}(Q) = 1 + \rho_0 \int_{\infty}^{0} 4\pi r^2 \{g_{ij}(r) - 1\}\frac{\sin(Qr)}{Qr}\mathrm{d}r \tag{2}$$

where $g_{ij}(r)$ is the averaged pair distribution function of j atoms found at a radial distance r from the position of atom i located at the origin and ρ_0 is the average number density of atoms. The corresponding pair distribution derived from $S^{obs}(Q)$, $g^{obs}(r)$ can also be described in the following form,

$$g^{obs}(r) \equiv \sum_{i,j} w_{ij}g_{ij}(r) = 1 + \frac{1}{2\pi^2 r\rho_0}\int_0^{\infty}\{S^{obs}(Q) - 1\}\sin(Qr)\mathrm{d}Q \tag{3}$$

It is emphasized that the observed structure factor $S^{obs}(Q)$ and its derived pair distribution function, $g^{obs}(r)$, involve the atomic scattering amplitudes of the constituents, while, neither the partial structure factors $S_{ij}(Q)$ nor their derivations $g_{ij}(r)$ involve any atomic scattering amplitudes.

The observed structure factor $S^{obs}(Q)$ for each alloy is shown in Figure 1. Cast a glance at these figures, there are several prominent tendencies in accordance with the concentration change. The first prominent feature in $S^{obs}(Q)$'s is that there form two peaks in the alloy of $c_{Te} = 0.5$ as if the ordinary first peak is split into two ones. And the same situation can be seen for the concentrations of $c_{Te} = 0.4$ and 0.6. Looking at these three $S^{obs}(Q)$'s, the second peak, or the sub-peak of the first peak suggests a strong correlation between Pb and Te atoms. The second prominent feature in $S^{obs}(Q)$'s is that the height of the peak beyond 40 nm^{-1} is gradually decaying with increasing the concentration c_{Te} from $c_{Te} = 0$ (i.e., pure liquid Pb) until $c_{Te} = 0.8$, although the total feature of $S^{obs}(Q)$ of pure Te is quite different from all other $S^{obs}(Q)$'s. The third feature, which is not so prominent, is that a very small swell in a small Q-region

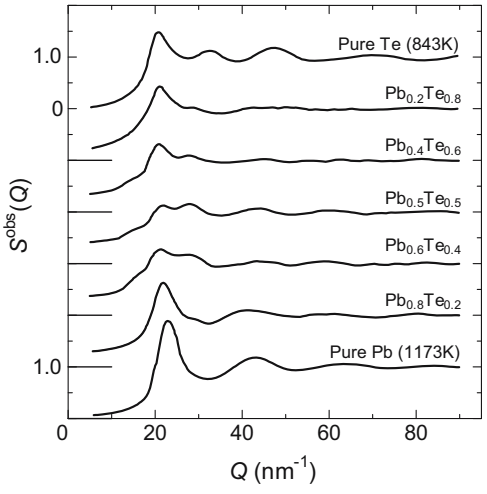

Figure 1: Observed total structure factors, $S^{obs}(Q)$'s, at various concentrations.

can also be seen for the alloys of c_{Te} = 0.4, 0.5 and 0.6, respectively.

In our previous paper, we have tried to obtain the partial $S_{ij}(Q)$ and thereby its corresponding $g_{ij}(r)$, by using these total structure factors, $S^{obs}(Q)$'s, of the alloys at the compositions of c_{Te} = 0.2, 0.4 and 0.5, respectively [6]. However, it is unable to reproduce either the observed $S^{obs}(Q)$ at c_{Te} = 0.5 by using these obtained partial structure factors. Presumably because of some sort of erroneous amount in the experimental results, the above treatment was insufficient to derive the exact partial structure factors $S_{ij}(Q)$. Therefore, we will hereafter try to derive newly the partial structure factors $S_{ij}(Q)$ by using all of measured data of $S^{obs}(Q)$ at c_{Te} = 0.2, 0.4, 0.5, 0.6 and 0.8, respectively. Using the coefficient w_{ij} defined as $w_{ij} = c_i c_j b_i b_j / b^2$, we can obtain the following determinant equation,

$$\boldsymbol{W} S_{ij}(Q) = S^{obs}(Q) \tag{4}$$

where $\boldsymbol{W}$ is a non-square matrix, defined as,

$$\boldsymbol{W} = \begin{bmatrix} w_{PbPb,c=0.2} & w_{PbTe,c=0.2} & w_{TeTe,c=0.2} \\ w_{PbPb,c=0.4} & w_{PbTe,c=0.4} & w_{TeTe,c=0.4} \\ w_{PbPb,c=0.5} & w_{PbTe,c=0.5} & w_{TeTe,c=0.5} \\ w_{PbPb,c=0.6} & w_{PbTe,c=0.6} & w_{TeTe,c=0.6} \\ w_{PbPb,c=0.8} & w_{PbTe,c=0.8} & w_{TeTe,c=0.8} \end{bmatrix}$$

$$S_{ij}(Q) = \begin{bmatrix} S_{Pb-Pb}(Q) \\ S_{Pb-Te}(Q) \\ S_{Te-Te}(Q) \end{bmatrix}$$

$$\text{and } S^{obs}(Q) = \begin{bmatrix} S_{c=0.2}(Q) \\ S_{c=0.4}(Q) \\ S_{c=0.5}(Q) \\ S_{c=0.6}(Q) \\ S_{c=0.8}(Q) \end{bmatrix}.$$

Putting the observed $S^{obs}(Q)$ into this equation, we can obtain the partial structure factors, $S_{ij}(Q)$ and thereby the partial pair distribution functions $g_{ij}(r)$'s are also derived, as shown in Figures 2 and 3. These figures are used for the fundamental data to proceed with the RMC (Reverse Monte Carlo) simulation, as shown in the next Section.

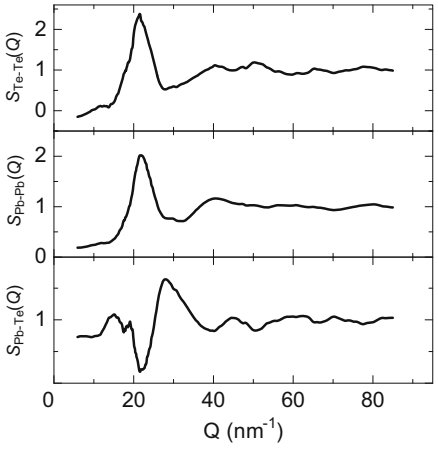

Figure 2: Estimated partial structure factors, $S_{ij}(Q)$'s (i, j = Pb and Te), by using $S^{obs}(Q)$'s.

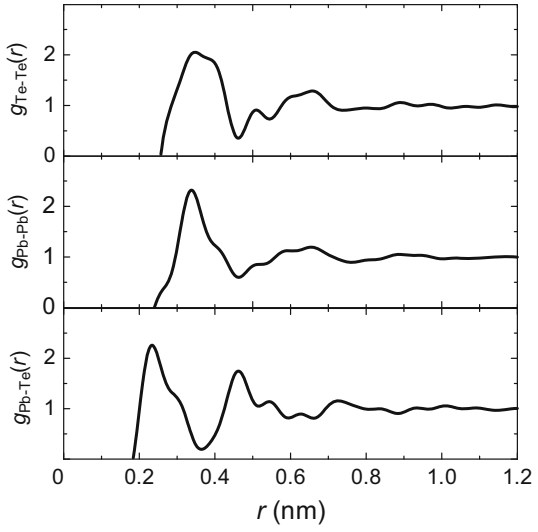

Figure 3: Estimated partial pair distribution functions, $g_{ij}(r)$'s, obtained from $S_{ij}(Q)$'s.

3 Reverse Monte Carlo simulation

The Reverse Monte Carlo (RMC) simulation, which was originally developed by McGreevy and his co-workers, is a useful procedure to illustrate spatially the short-range configuration of liquids, by analyzing the observed diffraction data [9]. And we here used the method of RMC simulation developed by Gereben and Pusztai [10]. A standard procedure of the Reverse Monte Carlo (RMC) simulation for a binary mixture will be briefly explained in what follows.

Let us consider a fixed cube in which the number density of atomic-type i and that of j are randomly involved, in order to carry out the RMC model. Taking that ρ_j is the number density of the type j atoms, then the partial pair distribution function $g_{ij}(r)$ is described as follows,

$$g_{ij}(r) = \frac{n_{ij}(r)}{4\pi r^2 \rho_j \Delta r} \tag{5}$$

where $n_{ij}(r)$ is the number of atoms of type j at a distance between r and $r + \Delta r$ from a central atom of type i, averaged over all atoms of the central type i.

The partial pair distribution functions in this RMC model, $g_{ij}^{RMC}(r)$'s and thereafter the partial structure factors $S_{ij}^{RMC}(Q)$'s are obtainable. And also the total structure factor $S^{RMC}(Q)$ can be derived, in which the weighing factors w_{ij}'s are involved.

A chosen number of the constituent atoms are moved randomly in the configuration, so as to close possibly the experimentally derived partial structure factors $S_{ij}(Q)$'s and then the total structure factor $S^{obs}(Q)$'s. Repeating these treatments, we are finally attainable to that $S_{ij}^{RMC}(Q)$'s and $S^{RMC}(Q)$ have, within the range of error bars, agreed with the observed $S_{ij}(Q)$'s $S_{ij}(Q)$'s and $S^{obs}(Q)$, respectively. The final three dimensional configuration is also obtainable.

A practical procedure for this treatment can be seen in the article described by Gereben and Pusztai [10].

Using the obtained partial structure factors from the observed total structures, $S_{Pb-Pb}(Q)$, $S_{Pb-Te}(Q)$ and $S_{Te-Te}(Q)$ obtained in the previous section, the RMC simulation is carried out for the liquid $Pb_{0.5}Te_{0.5}$, in order to obtain their three dimensional and short-range configurations. As per the RMC model, the cube of the length is equal to 5.621 nm, the particle numbers of Pb and Te atoms are equal to 2,312, respectively, which satisfies the experimental number density and initially the system was randomly distributed.

As seen in Figure 4, the RMC results, $S_{ij}^{RMC}(Q)$, are satisfactorily able to reproduce the experimentally derived partial structure factors $S_{ij}(Q)$ shown in Figure 2. In order to see the validity of the application of concentration method used for the derivation of $S_{ij}(Q)$'s, we have estimated the total structure factor $S^{RMC}(Q)$ of $Pb_{0.5}Te_{0.5}$ and compared with the experimentally observed total structure factor $S^{obs}(Q)$ at its composition.

Since the simulated total structure factor $S^{RMC}(Q)$ agrees completely with the observed $S^{obs}(Q)$ in liquid $Pb_{0.5}Te_{0.5}$, the application of concentration method to obtain the partial structure factors $S_{ij}^{RMC}(Q)$'s for the present system is therefore a reliable and useful technique.

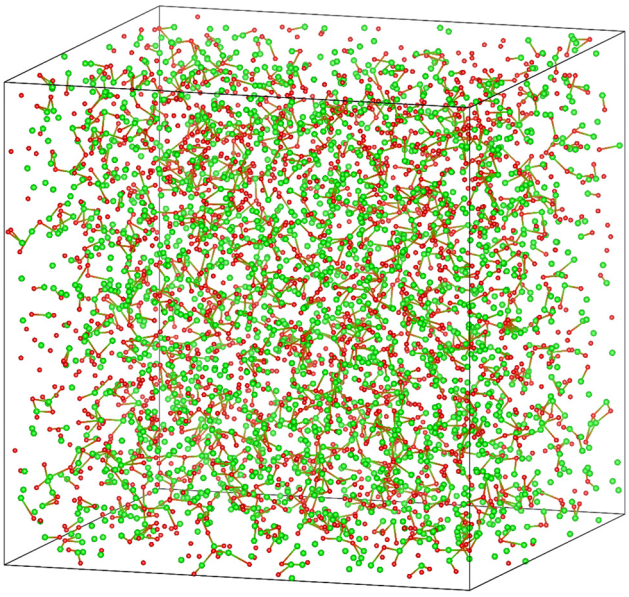

Figure 5: Picture of three dimensional configuration of liquid $Pb_{0.5}Te_{0.5}$ by using RMC simulation. Red and green indicate tellurium and lead, respectively. The covalent bonds indicated by a colored line between Te and Pb occur in the cases of $r \leqq 0.262$ nm.

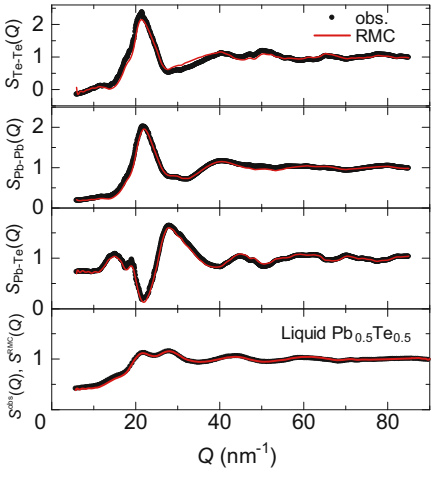

Figure 4: Reproduction of $S_{ij}^{RMC}(Q)$'s by using Reverse Monte Carlo simulation, and the comparison between the observed $S^{obs}(Q)$ of $Pb_{0.5}Te_{0.5}$ and the corresponding $S^{RMC}(Q)$ by the summation of $S_{ij}^{RMC}(Q)$'s.

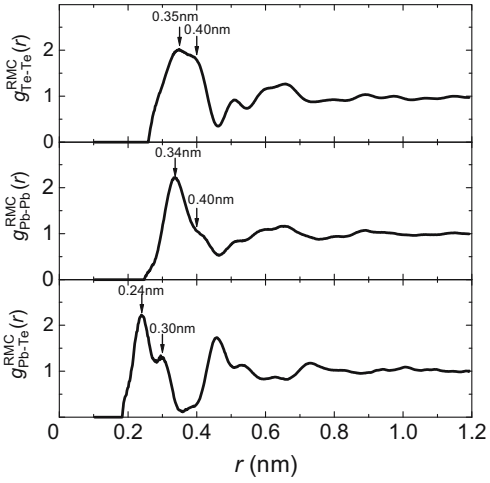

Figure 6: Partial pair distribution function $g_{ij}^{RMC}(r)$'s obtained from three dimensional configuration of $Pb_{0.5}Te_{0.5}$ by using RMC simulation.

The three dimensional atomic configuration for liquid $Pb_{0.5}Te_{0.5}$, obtained by RMC, is shown in Figure 5. It can be seen that there exists a lot of Pb–Te pairing, which might be caused by the remaining covalent-type molecular complex PbTe in the liquid state. The derived $g_{ij}^{RMC}(r)$'s from RMC simulation are shown in Figure 6. The partial pair distribution functions $g_{ij}^{RMC}(r)$'s by RMC simulation are obtained so as to reproduce the experimental ones, as shown in Figure 3. Looking at these $g_{ij}^{RMC}(r)$'s by RMC, we can discuss some short-range configurations in liquid $Pb_{0.5}Te_{0.5}$, which will be described in the next Section.

4 Information on the short-range structure in liquid Pb–Te alloys

Now we are in a position to determine the short-range configurations around Pb and Te atoms by using the partial pair distribution functions $g_{ij}(r)$'s described in Figure 3 or those in Figure 6. In this system, the averaged co-ordination number Z within the sphere of radius R, seen from one of the constituents located at the origin, is generally described as follows,

$$\begin{aligned} Z &= 4\pi\rho_0 \int_0^R g(r) r^2 \mathrm{d}r \\ &= 4\pi\rho_0 \int_0^R [c_{Pb}^2 g_{Pb-Pb}(r) + 2c_{Pb}c_{Te}g_{Pb-Te}(r) \\ &\quad + c_{Te}^2 g_{Te-Te}(r)] r^2 \mathrm{d}r \\ &= 4\pi\rho_0 \int_0^R [c_{Pb}\{c_{Pb}g_{Pb-Pb}(r) + c_{Te}g_{Pb-Te}(r)\} \\ &\quad + c_{Te}\{c_{Pb}g_{Pb-Te}(r) + c_{Te}g_{Te-Te}(r)\}] r^2 \mathrm{d}r \\ &= c_{Pb}\left[4\pi\rho_0 \int_0^R \{c_{Pb}g_{Pb-Pb}(r) + c_{Te}g_{Pb-Te}(r)\} r^2 \mathrm{d}r\right] \\ &\quad + c_{Te}\left[4\pi\rho_0 \int_0^R \{c_{Te}g_{Te-Te}(r) + c_{Pb}g_{Te-Pb}(r)\} r^2 \mathrm{d}r\right] \text{ or,} \\ &\equiv c_{Pb}Z_{Pb} + c_{Te}Z_{Te} \end{aligned} \tag{6}$$

We can take that the length of R is approximately equal to 0.40 nm, which is equal to the second minimum position of the total $g(r)$ in liquid $Pb_{0.5}Te_{0.5}$. Since the lowest minimum position of $g_{Pb-Te}(r)$ is equal around the position at $r \sim 0.36$ nm, the shape of total $g(r)$ is influenced by its contribution to yield the second minimum around $r = 0.40$ nm.

The physical meaning of Z_{Pb} is the co-ordination number within the sphere of radius R around a Pb atom located at the origin, and Z_{Te} means that around a Te atom. In the case of liquid $Pb_{0.5}Te_{0.5}$, Z_{Pb} is expressed as follows,

$$\begin{aligned} Z_{Pb} = Z_{Pb-Pb} + Z_{Pb-Te} &= 4\pi\rho_0(0.5)^2 \int_0^R g_{Pb-Pb}(r) r^2 \mathrm{d}r \\ &\quad + 4\pi\rho_0(0.5)^2 \int_0^R g_{Pb-Te}(r) r^2 \mathrm{d}r \end{aligned} \tag{7}$$

In a similar way, we have,

$$\begin{aligned} Z_{Te} = Z_{Te-Pb} + Z_{Te-Te} &= 4\pi\rho_0(0.5)^2 \int_0^R g_{Pb-Te}(r) r^2 \mathrm{d}r \\ &\quad + 4\pi\rho_0(0.5)^2 \int_0^R g_{Te-Te}(r) r^2 \mathrm{d}r \end{aligned} \tag{8}$$

Usually, the above method is utilized to know the information on the short-range atomic configuration in liquids, under the situation that $g_{ij}(r)$'s are known. However, the short-range pair distribution function $g_{Pb-Te}(r)$ has clearly two mountains up to 0.35 nm, and therefore the above method might be insufficient to know a detailed short-range configuration. Therefore, we wish to proceed with utilizing the results obtained by the RMC treatment in liquid $Pb_{0.5}Te_{0.5}$ in order to know their short-range configurations, in the next Section.

5 RMC method on the short-range configurations in liquid $Pb_{0.5}Te_{0.5}$

The obtained partial pair distribution functions shown in Figure 6 have very interesting features. In the case of $g_{Pb-Te}(r)$, there are two peaks within a short-range distance, up to $r = 0.35$ nm, as indicating two types of the nearest neighboring atom's contact. In other words, they are the first mountain of the peak position at $r = 0.24$ nm and the second one of the peak position at $r = 0.30$ nm, respectively. It must be plausible to consider that the first mountain might correspond to a group of the covalent-bond forming and the other one might correspond to a group of non-covalent bond forming, namely, forming a metallic mixture of Pb^{4+}, Te^{2+} and the

conduction electrons set free from constituent atoms in the mixture. The above inference seems to be acceptable, because the conduction electrons have a space to move among the constituent ions, while the inter-atomic distance must be smaller, in order to form a kind of covalent-type bonding. In fact, this inference can be deduced from the resistivity measurement [3].

There is a problem in how to assign the border between these two peaks. Although the minimum position is located at $r = 0.28$ nm, the first mountain is much more sharp than the second one, whose sharpness is naturally related to these peak heights of $g_{Pb-Te}(r)$, being as 2.20 and 1.25. In order to determine the real border position between these two mountains, the length between 0.24 nm and 0.30 nm should be divided by their inverse ratio of the sharpness or peak height of these mountains. Then we can decide that the border position is equal to 0.262 nm.

Using the three dimensional results of RMC simulation, we have estimated the number of Pb atoms around each Te atom, which is shown in Table 1. The coordination number zero in Table 1 means that there are 796 Te atoms around the sphere of these ones within the radius $r = 0.262$ nm that have no neighboring Pb atom at all. In other words, these Te atoms have no covalent-type bonding, and therefore they are constructing the metallic part. The ratio of 796 by 2,312 means that the fraction of metallic part is equal to 0.344 and therefore that of covalent-type bonding molecules is equal to 0.656. In view of the two mountains of pair distribution function $g_{Pb-Te}(r)$, the first one is the covalent-type bonding group and the second one corresponds to the metallic group. The fraction, 0.656, of covalent-type bonding formation given by the first mountain is just a comparable value of 0.64 obtained from the electrical resistivity measurement [3] and that of 0.665 obtained by the thermodynamic calculation [5]. The coordination number 1 in Table 1 means the formation of diatomic covalent-type molecule and its fraction is equal to (1,012/2,312) = 0.438, in comparison with the total number of Te atoms. The coordination number 2 in Table 1 means that some of the Te atoms have two neighboring Pb atoms as a configuration, indicating the tetrad covalent-type molecules, namely, the molecule of (2Pb–2Te) = {2(PbTe)} forms a kind of square. And the fraction of Te atoms forming this square is equal to (409/2,312) = 0.177, in comparison with the total number of Te atoms. The coordination number 3 might be understandable by that the group of {4(PbTe)} forms, for example, a kind of cubic structure, although its fraction is very minor, being equal to 0.038. Therefore, in the three dimensional data obtained by the present RMC simulation in liquid $Pb_{0.5}Te_{0.5}$, there exist various types of the covalent-type bonds, forming randomly one dimensional dipoles, two dimensional tetrads and three dimensional cubes, as shown in Figure 7.

Table 1: Number of bonded coordination around each Te atom and number of Pb atoms belonging to its group

Number of bonded coordination around each Te atom	Number of Pb atoms belonging to its group
0	796
1	1,012
2	409
3	87
4	9
	Total number = 2,312

Now we will investigate the cases of $g_{Pb-Pb}(r)$ and $g_{Te-Te}(r)$ in what follows. In the case of $g_{Pb-Pb}(r)$ up to $r = 0.46$ nm, the mountain has the maximum at the position $r = 0.34$ nm and a shoulder around $r = 0.40$ nm, which fact seems to be an overlapping of two mountains. The existence of these two mountains seems to be natural. On one hand, in the group of mountains at the peak position of $r = 0.46$ nm, a Pb atom is located at the position of the other neighboring Pb atom, which is used for the formation of the covalent forming molecule. On the other hand, in the group of mountains at the peak position around = 0.40 nm, both Pb atoms might belong to a metallic region. The difference in these peak positions in the pair distribution function, $g_{Pb-Pb}(r)$, can be ascribed to the difference in their inter-atomic potentials. In the mountain group of the peak position at = 0.34 nm, the main inter-atomic potential is caused by the interaction between the ionized Pb^{4+} ion and the electric dipole (or multipole etc.) through the conduction electrons, which seems to be smaller than the inter-ionic potential between Pb^{4+} ions through the conduction electrons, and naturally the inter-atomic distance becomes longer.

In a similar way, we can analyze the case of $g_{Te-Te}(r)$ up to $r = 0.47$ nm. The mountain has the maximum at the position $r = 0.35$ nm and a gradual shoulder around $r = 0.40$ nm, which situation seems to be an overlapping of two mountains. In the group of mountains of $g_{Te-Te}(r)$ at the peak position of $r = 0.35$ nm, in which one of the Te atoms belonging to a pair of Te–Te may be used for the formation of the covalent forming molecule. On the other hand, in the group of mountains at the peak position around $r = 0.40$ nm, both Te atoms might belong to a metallic region.

In Table 2, we summarize all the partial coordination numbers in liquid $Pb_{0.5}Te_{0.5}$. The characteristic feature is, therefore, that the neighboring inter-atomic distance is

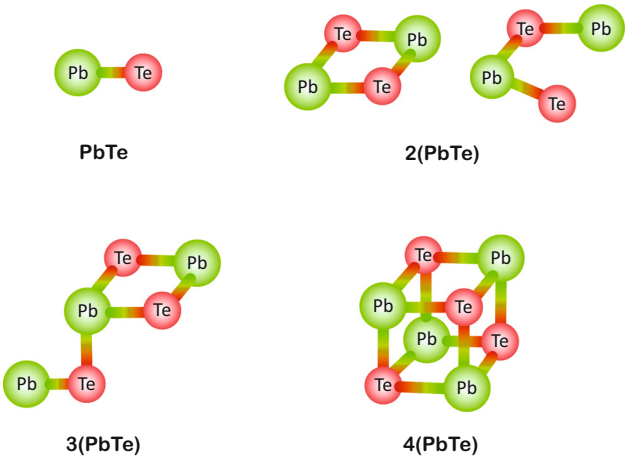

Figure 7: Possible examples of the covalent-type molecules, PbTe, 2(PbTe), 3(PbTe) and 4(PbTe).

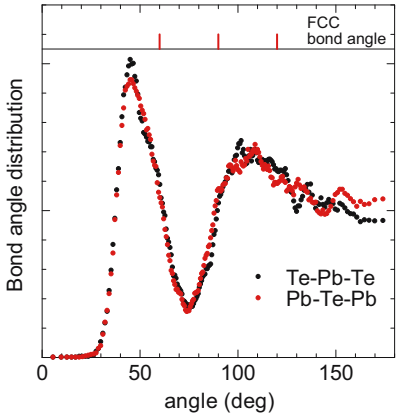

Figure 8: Bond angle distributions in liquid $Pb_{0.5}Te_{0.5}$ obtained from three dimensional configuration of $Pb_{0.5}Te_{0.5}$ by using RMC simulation.

relatively shorter than that of solid semiconductor PbTe, and that the coordination numbers around the constituent atoms are smaller than six coordination as in the solid state. Using Table 2, we can estimate the averaged numbers of nearest neighboring atoms around either an arbitrary atom, Pb or Te. The averaged number around Te atom forming a covalent-type molecule is equal to (1.4 + 2.9) = 4.3 and that forming a metallic region is equal to (1.3 + 2.6) = 3.9, respectively. Therefore, both averaged numbers around Te atom are about four, which is certainly smaller than the nearest neighbor's number of solid PbTe which is equal to six.

6 Bond angle distribution in liquid $Pb_{0.5}Te_{0.5}$ by using RMC configuration

The bond angle distributions in liquid $Pb_{0.5}Te_{0.5}$ are also estimated by using the three dimensional configuration of $Pb_{0.5}Te_{0.5}$ by using RMC simulation, in order to make sure whether any small but local group of the solid NaCl-type structure remains or not. In order to identify the existence of such a solid NaCl-type structure, it is necessary that the numbers of Pb and Te must be, at least, required more than 14, respectively. However, the three dimensional covalent-type molecule in liquid $Pb_{0.5}Te_{0.5}$ seems to be a cube of 4(PbTe), which is too small in comparison with the unit of NaCl-type crystal. As seen in Figure 8, distributions of bond angles tell us no apparent agreement with the solid-type FCC bond angles, which has resulted from that either Pb atoms or Te ones in their solid type form the FCC structure, respectively.

Furthermore, we have tried to construct the Voronoi polyhedron to ascertain whether there exists any special polyhedron or not [11]. And results tell us that there is no existence of any particular polyhedron indicating a short-range crystalline structure. Then the packing fraction becomes small and the constituent atoms are randomly distributed in the three dimensional space.

Table 2: Partial co-ordination numbers in liquid $Pb_{0.5}Te_{0.5}$ by three dimensional RMC

Pair	Average length/nm	Co-ordination number, *Z*	Total fraction (%)	Total fraction (%) thermodynamic	Total fraction (%) electrically
Pb–Te (covalent)	0.24	1.40 ± 0.15	65.6	66.5	64.0
Pb–Te (metallic)	0.30	1.30 ± 0.15	34.4		
Pb–Pb (cov.–met.)	0.34	2.79 ± 0.25			
Pb–Pb (met.–met.)	0.40	2.85 ± 0.40			
Te–Te (cov.–met.)	0.35	2.90 ± 0.20			
Te–Te (met.–met.)	0.40	2.60 ± 0.25			

7 An explanation for the short-range structure in liquid $Pb_{0.5}Te_{0.5}$

It is known that the solid $Pb_{0.5}Te_{0.5}$ has a rock salt type structure with mainly a covalent-bonding nature, as one of the narrow gap semiconductors, and its lattice constant is equal to 0.646 nm, that is, the nearest neighboring distance between Pb and Te atoms is equal to 0.323 nm. On melting of this solid $Pb_{0.5}Te_{0.5}$, there occurs a small volume expansion like the same phenomenon in a usual solid–liquid transition. Naturally, this material in its liquid state, the number of nearest neighboring becomes smaller than six, as shown in the previous sections. Liquid $Pb_{0.5}Te_{0.5}$ has therefore three distinct properties, as follows.

1) Under the present situation, we have found that the nearest neighboring configuration for Pb–Te pairing in liquid $Pb_{0.5}Te_{0.5}$, $g_{Pb-Te}(r)$ has two peaks at 0.24 nm and 0.30 nm. The ratio of $Z_{Pb-Te}(0.24\,nm)$ to $Z_{Pb-Te}(0.30\,nm)$ is approximately equal to 2:1. As described in the former sections, the short length at 0.24 nm can be understandable by a local formation of covalent bond. The electronic ground states of Pb and Te atoms are given by $Pb(4f^{14}5d^{10}6s^26p^2)$ and Te $(4d^{10}5s^25p^4)$, respectively. The outer electron's configurations of these atoms are fundamentally similar to atoms of $C(2s^22p^2)$ and $O(2s^22p^4)$, respectively, which form a covalent-bonding CO composed of two ordinary covalent bonds and one dative bond.
2) A rather short length such as 0.24 nm is never explained by the ionic bonding between Pb^{2+} and Te^{2-} ions, because the Pauling's ionic radii of Pb^{2+} and Te^{2-} are 0.133 nm and 0.207 nm, respectively, and thus a reliable inter-ionic distance of ionic pair $Pb^{2+}Te^{2-}$ might be equal to around 0.34 nm.
3) According to the electrical resistivity, this liquid system is evidently given by a mixture of some of the covalent-type molecules and the metallic region composed of positive Pb ions, positive Te ions and conduction electrons set free from these Pb and Te atoms [3,12].
4) The metallic fraction of this system is going to increase with temperature [3]. Taking that the required energy from the covalent-type bonding to the metallic one is equal to E_{vm}, then the metallic fraction is given by $\{\exp(-E_{vm}/RT)\}$. Since the present result finds out that the metallic fraction at 1,200 K is approximately equal to (1/3), the estimated E_{vm} is equal to 11.0 kJ/mol. As seen in Table 1, the existing fraction of the covalent complex is equal to (2/3) and the metallic fraction is (1/3), respectively. This kind of co-existence of the covalent PbTe molecules and the metallic remains makes it possible to exchange from the covalent molecules to the metallic state or vice versa, under the condition of thermodynamic equilibrium. Accompanying with this situation, the lifetime of the covalent molecules of PbTe in the system must be finite, as discussed below.
5) The lifetime can be estimated as the dissociation of covalent diatomic molecule PbTe. According to a review article written by Hänngi et al. [13], the reaction rate in relation to this dissociation, under the approximation of harmonic potential model for bonding, is given by the following equation,

$$\frac{1}{\tau} = \left(\frac{r_b}{r_0}\right)^2 \frac{\omega_0}{2\pi} \exp\left(-\frac{E_{vm}}{RT}\right) \tag{8}$$

where τ means the lifetime or the relaxation time of the diatomic molecule, and r_b is equal to the length where the bonding is broken, r_0 the bond length, ω_0 the angular frequency of vibration and E_{vm} the energy for its dissociation, as discussed above. Taking $r_b \sim 0.27$ nm, $r_0 \sim 0.24$ nm, $\omega_0 = 10^{13}\ s^{-1}$ (as an assumption as the same order of the lattice vibration), $E_{vm} \sim 11.0$ kJ/mol and $T = 1,200$ K, we have the lifetime τ as being equal to 1.5×10^{-12} s, that is, about 15 times of vibration makes it possible to dissociate the covalent bond from the metallic one.

8 Discussion

Gierlotka et al. have insisted that a complex of Pb^{2+} and Te^{2-} ions is stable in liquid Pb–Te alloys, and by using the ionic model, they have explained the mixing enthalpies and Gibbs free energies of mixing in liquid Pb–Te alloys [14]. However, if we accept this concept, then at least there forms a mixture of metallic lead and the molten salt of $Pb^{2+}Te^{2-}$ in the alloy with the condition of $0 < c_{Te} < 0.5$. In view of a common sense, this situation is very difficult to exist stably in one phase, because the mixture of molten salt and liquid metal exhibits the two phase separation. In particular, if we assume that the bonding character of liquid $Pb_{0.5}Te_{0.5}$ is a mixture of Pb^{2+} ions and Te^{2-} ions, which situations were proposed by Gierlotka et al., then the closest inter-ionic distance must be close to about 0.341 nm, which is obtainable from the Pauling's ionic

radius of Pb^{2+} equal to 0.120 nm and that of Te^{2-} is 0.221 nm. However, the closest inter-atomic distance between Pb and Te atoms observed in the present investigation is located at $r = 0.24$ nm, which result completely contradicts the ionic model.

Although we could not distinguish the concrete forming shape of the liquid lead telluride PbTe at the time we had measured the resistivity of this system, its forming shape can be, under the present investigation, cleared out as the covalent molecular complex, as shown in Figure 7. Since the solid thin film (300 nm) of lead telluride PbTe has the value of about 1.5×10^{-3} Ωm in its electrical resistivity at room temperature [15], the electrical resistivity in its bulk crystal must be of the same order or smaller than its value. If liquid $Pb_{0.5}Te_{0.5}$ is mainly exhibited by a molten salt, then we can guess its electrical resistivity as the order of $10^{-3} \sim 10^{-2}$ Ωm. However, the real electrical resistivity in liquid $Pb_{0.5}Te_{0.5}$ is the order of 8.0 μΩ m, which value can often be seen in ill-conditioned liquid metals and alloys. Therefore, the electrical resistivity data indicate that the molten $Pb_{0.5}Te_{0.5}$ cannot be explained in terms of molten salt at all.

It is therefore concluded that molten $Pb_{0.5}Te_{0.5}$ is a mixture of covalent-type complexes of the molecules PbTe, 2(PbTe), 3(PbTe) and 4(PbTe), and the metallic remains composed of the positive ions of Pb^{4+}, Te^{2+} and the conduction electrons being set free, which concept was already concerned in our previous report [3].

Under this situation, it is inferred that all liquid $Pb_{1-c}Te_c$ $(1 > c = c_{Te} > 0)$ alloys are also mixtures of covalent-type molecules of PbTe and the metallic part which is provided from the remains of Pb and Te atoms.

Acknowledgments: We are grateful to Emeritus Professor Y. Waseda of Tohoku University and Professor T. Ishiguro of Tokyo University of Science for their valuable comments and discussions.

References

[1] Ravich, Yu. I., B. A. Efimova, and I. A. Smirnov. *Semiconducting Lead Chalcogenides*. Plenum Press, New York, 1970.

[2] Takeda, S., Y. Tsuchiya, and S. Tamaki. Magnetic susceptibilities of liquid Pb–Te alloys. *Journal of the Physical Society of Japan*, Vol. 45, 1978, pp. 479–483.

[3] Takeda, S., T. Akasofu, Y. Tsuchiya, and S. Tamaki. Compound-forming effect for the electronic properties of liquid Sn–Te alloys. *Journal of Physics F: Metal Physics*, Vol. 13, 1983, pp. 109–117.

[4] Akasofu, T., S. Takeda, and S. Tamaki. Compound-forming effect in the electrical resistivity of liquid Pb–Te alloys. *Journal of the Physical Society of Japan*, Vol. 52, 1983, pp. 2485–2491.

[5] Akasofu, A., M. Kusakabe, and S. Tamaki, An interpretation on the thermodynamic properties in liquid Pb–Te alloys. *High Temperature Materials and Processes* (in press), DOI: 10.1515/htmp-2020-0068.

[6] Takeda, S., K. Iida, S. Tamaki, and Y. Waseda. The structure of liquid Pb–Te alloys by neutron diffraction. *Bulletin of the College of Biomedical Technology Niigata University*, Vol. 1, 1983, pp. 30–37.

[7] Bacon, G. E. Coherent neutron scattering amplitudes. *Acta Crystallographica, Section A: Crystal Physics, Diffraction, Theoretical and General Crystallography*, Vol. 28, 1972, pp. 357–358.

[8] Halder, N. C., and C. N. J. Wagner. Partial interference and atomic distribution functions of liquid silver—tin alloys. *Journal of Chemical Physics*, Vol. 47, 1967, pp. 4385–4391.

[9] McGreevy, R. L., and L. Pusztai. Reverse monte carlo simulation: a new technique for the determination of disordered structures. *Molecular Simulation*, Vol. 1, 1988, pp. 359–367.

[10] Gereben, O., and L. Pusztai. RMC_POT: a computer code for reverse monte carlo modeling the structure of disordered systems containing molecules of arbitrary complexity. *Journal of Computational Chemistry*, Vol. 33, 2012, pp. 2285–2291.

[11] Rycroft, C. VORO++: a three-dimensional Voronoi cell library in C++. *Chaos*, Vol. 19, 2009, pp. 041111–1.

[12] Enderby, J. E. Structure and electronic properties of liquid semiconductors (Chapter 7). In *Amorphous and liquid semiconductors*, Tauc, J., Eds, Springer US, New York, 1974, pp. 361–433.

[13] Hänngi, P., P. Talkner, and M. Borkovec. Reaction-rate theory: fifty years after Kramers. *Reviews of Modern Physics*, Vol. 62, 1990, pp. 251–341.

[14] Gierlotka, W., J. Łapsa, and D. Jendrzejczyk-Handzlik. Thermodynamic description of the Pb–Te system using ionic liquid model. *Journal of Alloys and Compounds*, Vol. 479, 2009, pp. 152–156.

[15] Abd El-Ati, M. I. Electrical conductivity of PbTe thin films. *Physics of the Solid State*, Vol. 39, 1997, pp. 68–71.